

RSC Advances



This is an *Accepted Manuscript*, which has been through the Royal Society of Chemistry peer review process and has been accepted for publication.

Accepted Manuscripts are published online shortly after acceptance, before technical editing, formatting and proof reading. Using this free service, authors can make their results available to the community, in citable form, before we publish the edited article. This *Accepted Manuscript* will be replaced by the edited, formatted and paginated article as soon as this is available.

You can find more information about *Accepted Manuscripts* in the [Information for Authors](#).

Please note that technical editing may introduce minor changes to the text and/or graphics, which may alter content. The journal's standard [Terms & Conditions](#) and the [Ethical guidelines](#) still apply. In no event shall the Royal Society of Chemistry be held responsible for any errors or omissions in this *Accepted Manuscript* or any consequences arising from the use of any information it contains.



Rapid growth of large size, highly deuterated DKDP crystal and its efficient noncritical phase matching fourth-harmonic-generation of Nd:YAG laser

Received 00th January 20xx,
Accepted 00th January 20xx

DOI: 10.1039/x0xx00000x

www.rsc.org/

Lisong Zhang,^{a, b} Fang Zhang,^{a, b} Mingxia Xu,^{a, b} Zhengping Wang,^{a, b, *} Xun Sun^{a, b, *}

High quality, large sizes ($100 \times 105 \times 96 \text{ mm}^3$) deuterated potassium dihydrogen phosphate (DKDP) crystal with high deuterium content was successfully grown by the rapid growth method. The noncritical phase matching (NCPM) fourth-harmonic-generation (FHG) of Nd:YAG laser (1064 nm) were realized at 39.7 °C or so. The smallest full width at half maximum (FWHM) of angular acceptance for the longest crystal sample (20 mm) is 33.5 mrad, which is 10 times larger than the value of critically PM of KDP crystal. The FHG conversion efficiency increases with the crystal length and reaches 64% for the 20 mm long crystal. As we have known, it is the highest FHG conversion efficiency of 1064 nm laser with a repetition rate of 10 Hz in low drive condition.

Introduction

Deep ultraviolet (UV) coherent light is desirable for precise material processing.^{1,2} Due to its short wavelength and high peak power, it can achieve extremely small feature sizes down to less than one micrometer with great precision. What is more, coherent light in the UV range can avoid the thermal effect made by infrared or visible laser and permit the non-thermal ("cold") processing. On the other hand, UV laser can be widely used for spectroscopy and other fields.

The noncritical phase matching (NCPM) fourth-harmonic-generation (FHG) of 1 μm laser is one of the most useful methods to obtain deep UV coherent light with high efficiency. KDP type crystals can realize NCPM FHG in 1050-1070 nm wavelength range.³⁻¹⁵ Among them, the preferable candidates are considered to be 60% deuterium content DADP and 70% deuterium content DKDP, which can realize room temperature NCPM FHG of 1053 nm laser with extremely high conversion efficiency.^{11,13} ADP crystal and its 60% deuterium content isomorphs are sensitive to temperature and has a narrow temperature full width at half maximum (FWHM) due to the high thermo-optical effect.¹⁶⁻²⁰ This characteristics is advantageous and can be widely used in optical parametric oscillation (OPO) domain. However in NCPM FHG domain, it limits the application of ADP (DADP) crystals. Because it requires wide temperature FWHM in NCPM FHG in order to simplify the temperature requirement. Although 70% DKDP crystal has a wide temperature FWHM, it is sensitive to deuterium content. It is hard to grow homogeneous, medium deuterium content DKDP crystals, especially by rapid growth method. Highly deuterium content DKDP crystal is one of the solutions to overcome both the narrow

temperature FWHM and the deuterium content inhomogeneity. Although highly deuterium content DKDP crystal is not suitable for 1053 nm Nd:glass laser because its NCPM temperature is far below the room temperature, it is welcomed by the NCPM FHG of commercial 1064 nm Nd:YAG laser.

In this paper, large sizes, highly deuterium content DKDP crystal was grown by rapid growth method. The crystal quality was examined, and its high efficiency NCPM FHG of 1064 nm laser was demonstrated.

Crystal growth

The DKDP crystal was grown from highly deuterium content DKDP solution. The solution was synthesized by electronic pure grade P_2O_5 , anhydrous K_2CO_3 and D_2O with deuterium content $\geq 99.8\%$. The synthesis process is same as reference 21. To avoid hydrogen-deuterium exchange, synthesis process was conducted under dry ambient, in which the humidity was kept below 20%. Saturated temperature of the solution was adjusted to 55 °C and the pH value was set to 3.9. The solution was filtered through a 0.1 μm filter and then overheated at 75 °C for more than 72 hours. Crystallization was performed in a 20 L holden-type crystallizer with a temperature control accuracy of ± 0.1 °C. The DKDP crystal was grown by point-seed rapid growth method, and the temperature decreased from 55 to 40 °C in 15 days. The sizes of the as-grown crystal were $100 \times 105 \times 96 \text{ mm}^3$ without visible macroscopic defect, as shown in Figure 1.

Crystal quality

To examine the quality of the crystal, a measurement of refractive index inhomogeneity was conducted on a Z-cut sample. Figure 2 shows the inhomogeneity map for the whole cross-section. As a common phenomenon in rapid grown crystals, the sector boundaries between the prism area and pyramid area can be observed. The veins at the bottom of the map are caused by

^a. State Key Laboratory of Crystal Materials, Shandong University Jinan 250100, China. E-mail addresses: sunxun@sdu.edu.cn Tel./fax: +86 53188365200

^b. Key Laboratory of Functional Crystal Materials and Device (Shandong University), Ministry of Education Jinan 250100, China

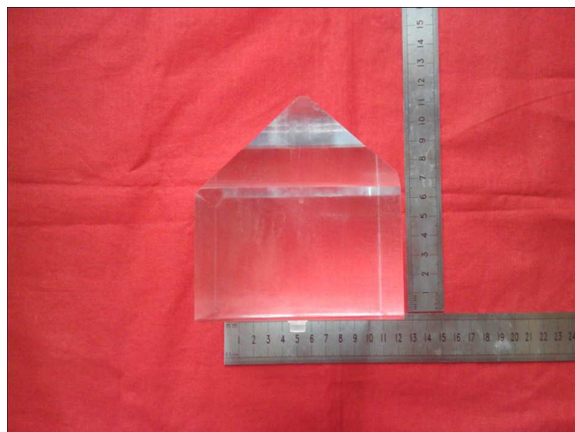


Figure 1. As-grown DKDP crystal with dimensions of $100 \times 105 \times 96 \text{ mm}^3$.

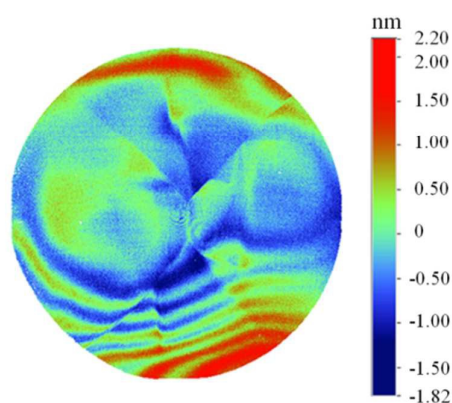


Figure 2. Refractive index inhomogeneity map of as-grown DKDP crystal.

machining processing rather than crystal defect. Although there are sector boundaries and machining veins, the overall refractive index inhomogeneity is only 0.441 ppm. It indicates that the quality of the crystal is pretty good. The sector boundaries can be alleviated by improving crystal growth techniques. Generally, for a rapid grown DKDP crystal, the crystal quality in pyramid area is much better than that in prism area. So we selected all of the FHG samples from the pyramid area.

FHG experiments

The fundamental light source is a commercial PY61 Nd:YAG laser with a wavelength of 1064 nm, pulse width of 40 ps, and repetition rate of 10 Hz. The experimental setup is shown in Figure 3. The fundamental laser was firstly converted to 532 nm by a 30 mm thick, $(41^\circ, 45^\circ)$ -cut, type-I PM SHG KDP crystal. To conduct FHG experiment, a series of different length DKDP crystals with an aperture of $10 \times 10 \text{ mm}^2$ were $(45^\circ, 90^\circ)$ -cut for type-I NCPM FHG. All of these samples were cut from the pyramid area of the large DKDP boule. Locations of each sample with respect to as grown crystal are shown in Figure 4. The transmittance faces of the samples were fine polished to reduce the back reflection at the crystal surfaces. DKDP sample is placed in a sealed but two sides transparent copper chamber to control the crystal temperature in an accuracy of 0.05°C . The DKDP crystal together with the copper chamber can rotate within a plane parallel to its optical axis and the rotate angle can be controlled precisely by a SC300 stepper motor controller. Firstly, temperature tuning experiment was conducted with the DKDP crystal fixed at its collimation position to determine the best NCPM temperature. Then angle tuning experiment was conducted by control the crystal temperature at T_{NCPM} to determine the angular acceptance. At last, NCPM FHG conversion efficiency was determined at different 2ω intensities.

Results and discussion

Temperature tuning

Previous reports showed that DKDP could realize NCPM at about 60°C . It is still inconvenient for practical use. Our experiment shows that the NCPM temperature decreases with the increase of deuterium content. For 99% deuterium DKDP, NCPM can be realized at near room temperature. For nonlinear optical (NLO) crystal, it is preferable to have large temperature bandwidth in

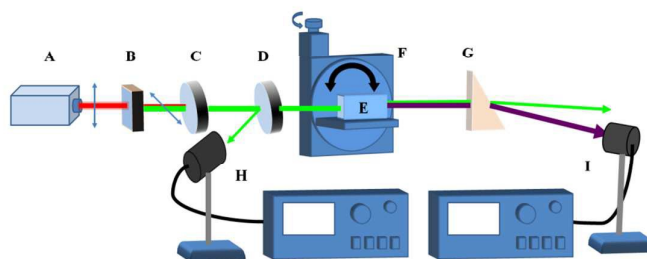


Figure 3. Experimental setup for the NCPM FHG. A. 1064-nm fundamental laser; B. SHG KDP crystal, C, D. beam splitters; E. FHG DKDP crystal; F. motorized rotation stage; G. CaF_2 prism; H, I. energy calorimeters.

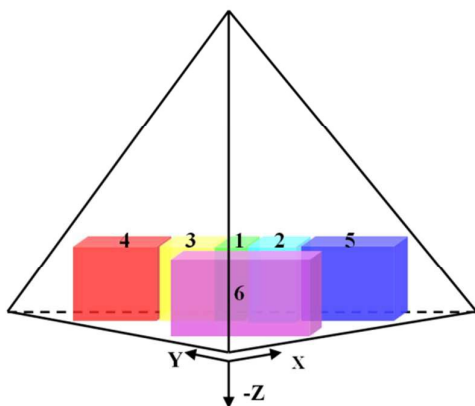


Figure 4. Cutting schematic diagram of different length DKDP samples from the pyramid area of the as-grown crystal. 1, 4 mm; 2, 6 mm; 3, 8 mm; 4, 12 mm; 5, 14 mm; 6, 20 mm.

order to reduce the requirement of temperature controlling. Figure 5 shows the FHG temperature tuning curves of different length DKDP crystals. The curves are fitted by the function of $\sin^2 x/x^2$ to determine the T_{NCPM} and the FWHM of the curve. The measured T_{NCPM} and the FWHM are listed in Table 1. The NCPM temperatures of different length crystals are found to be 39.45 ~ 40 °C. It indicates that the deuterium content of the crystal is 98.6 ~ 98.9%, which is almost the highest which can be obtained from DKDP solution. It is obvious that the temperature acceptance decreases roughly with the inverse of the crystal length. For the 20 mm long DKDP crystal, the measured FWHM temperature bandwidth is

1.34 °C, corresponding to a temperature bandwidth of 2.68 °C·cm and a temperature phase-mismatch sensitivity, $\partial\Delta k/\partial T$, of 2.08 °C⁻¹·cm⁻¹. These results are similar to Steven T. Yang's.¹¹ Theoretically, the temperature phase-mismatch sensitivity is independent with the crystal length. However, our results show that $\partial\Delta k/\partial T$ varies in 2 ~ 4 °C⁻¹·cm⁻¹ for different samples. The reason is that above method used to evaluate $\partial\Delta k/\partial T$ is not accurate enough.²²

Due to the isotope effect, the effective segregation coefficient K_{eff} is less than 1.²³ Thus the deuterium content of DKDP crystal is lower than the deuterium content of solution. What is more complicated, K_{eff} will be affected by crystal growth conditions such as temperature, supersaturation, and hydrodynamics, which lead to the deuterium content inhomogeneity in the as-grown crystal. Generally, the deuterium content of DKDP crystal will decrease gradually with the growth procedure. Thus the deuterium content at the boundary of the as-grown crystal will be lower than that in the centre of the as-grown crystal, which leads to higher NCPM temperature. It agrees well with our experimental results. NCPM temperatures of the samples far from crystal center (4#, 5#) are higher than those near crystal center (1#, 2#, 3#, 6#). Considering the relative locations of each sample with respect to as grown crystal, the deuterium gradient is estimated to be 0.14%/cm. This deuterium gradient can be extrapolated to the whole cross-section of as grown DKDP crystal. Figure 6 shows the deuterium gradient schematic diagram of the DKDP crystal. Its distribution trends are in agreement with the crystal growth procedure of rapid growth method. The deuterium content inhomogeneity will decrease the conversion efficiency of NCPM FHG because T_{NCPM} is sensitive to deuterium content. Our previous research showed that it caused 0.59%/cm deuterium gradient in DKDP crystal grown from 75% deuterium content DKDP solution.²⁴ For our as grown highly deuterated DKDP crystal, the deuterium gradient is much lower than the 75% deuterium content situation. It is because the

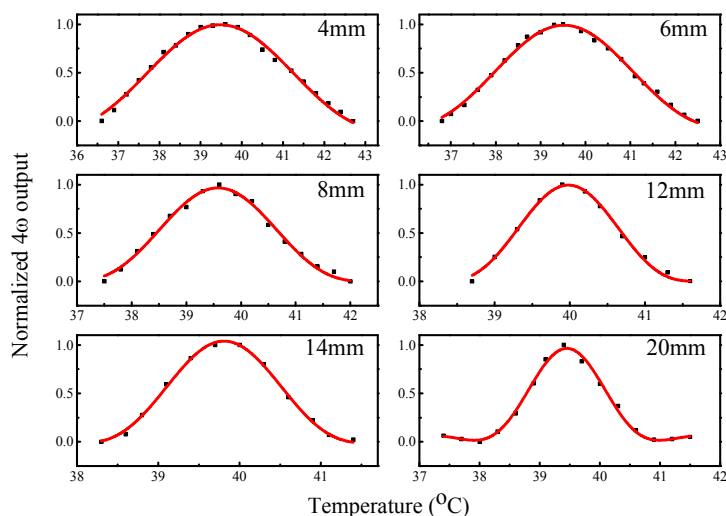


Figure 5. Temperature tuning curves of different length DKDP crystals. The black dots are experimental data and the solid color lines are fitted by $\sin^2 x/x^2$

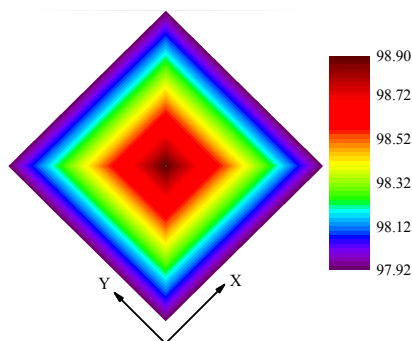


Figure 6 Deuterium gradient schematic diagram of as grown DKDP crystal.

effective segregation coefficient K_{eff} is closer to 1 in highly deuterium content solution, which decreases the deuterium content inhomogeneity. Low deuterium gradient in highly deuterium content DKDP crystal makes it possible to produce high quality, large size optical devices, which can be widely used in large size Nd:YAG lasers.

Angle turning

One of the advantages under NCPM condition is the wide angular acceptance, which reduces the requirement of beam quality. To study the angle tuning property, experiments were conducted by monitoring the fourth harmonic output as the crystal is rotated around its collimation position in θ direction, when the crystal temperature is fixed at T_{NCPM} . Figure 7 shows the angle turning curve of different length DKDP crystals. The curves were fitted by $\sin^2 x/x^2$ to determine the FWHM of angular acceptance and calculate the second order angular phase-mismatch sensitivities, $\partial^2 \Delta k / \partial (\Delta \theta)^2$. The results for different length DKDP crystals are also listed in Table 1. It is obvious that the long crystal corresponds to small angular acceptance. Theoretically, $\partial^2 \Delta k / \partial (\Delta \theta)^2$ is

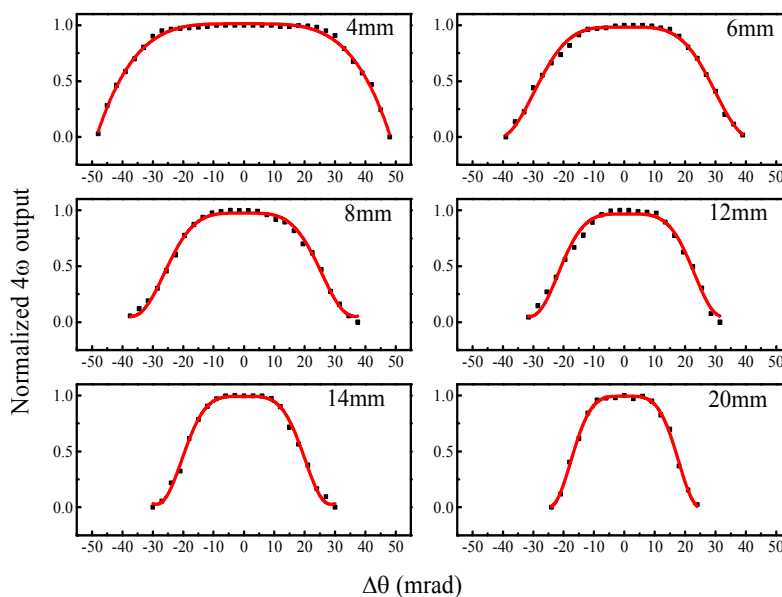


Figure 7. Angle turning curve of different DKDP crystals. The black dots are experimental data and the solid red lines are fitted by $\sin^2 x/x^2$.

Table 1. NCPM FHG properties of different length DKDP samples.

Crystal No.	T_{NCPM} ($^{\circ}\text{C}$)	Crystal length (cm)	ΔT ($^{\circ}\text{C}$)	$\partial \Delta k / \partial T$ ($^{\circ}\text{C}^{-1} \text{cm}^{-1}$)	$\Delta \theta$ (mrad)	$\partial^2 \Delta k / \partial (\Delta \theta)^2$ ($\times 10^3 \text{mrad}^{-2} / \text{cm}$)
1	39.48	0.4	3.53	3.94	81.67	8.34
2	39.52	0.6	3.12	2.97	55.98	11.84
3	39.58	0.8	2.25	3.09	49.62	11.30
4	39.98	1.2	1.42	3.27	42.81	10.12
5	39.80	1.4	1.54	2.58	38.62	10.66
6	39.45	2.0	1.34	2.08	33.53	9.90

independent with crystal length, and angular acceptance will decrease roughly as the inverse square root of the crystal length. The data of $\partial^2 \Delta k / \partial (\Delta \theta)^2$ in table 1 is accordant with this discipline which are unchanged basically. The smallest FWHM of angular acceptance is 33.53 mrad, which comes from the longest crystal (20 mm). Even so, this value is still 10 times larger than that of critically phase-matched KDP crystal.

Conversion efficiency

There is no beam walk-off under NCPM condition and the FHG conversion efficiency will increase with the crystal length. Figure 8 shows the relationship between conversion efficiency and crystal length. The conversion efficiency of 26 mm crystal was obtained by sticking 20 mm and 6 mm crystals together. It shows that the FHG conversion efficiency will increase with the crystal length and then reach a flat top when the crystal is longer than 20 mm. Under NCPM condition, the FHG conversion efficiency strongly depends on the UV absorption of the crystal. It is reported that nonlinear absorption coefficient during FHG in DKDP crystal can be neglected in low 2ω drive level ($\leq 1 \text{ GW/cm}^2$).¹¹ Thus in our experiment performed in low drive level, the only restriction to conversion efficiency is the linear absorption coefficient. When crystal is longer than 20 mm, the energy loss caused by linear absorption will deplete the energy gain and the conversion efficiency will reach a flat top. It means that for present experimental conditions the best crystal length for NCPM FHG is 20 mm or so. By adjusting the intensity of the 2ω beam (532 nm), we measured the variation of the FHG conversion efficiency for the 20 mm crystal. As shown in Figure 9, the FHG conversion efficiency increases with the 2ω intensity. It becomes saturated when the 2ω intensity is beyond 0.2 GW/cm^2 . The highest conversion efficiency is 64%. Taking the 4% Fresnel reflection loss at each uncoated crystal surface into consideration, the actual conversion efficiency inside the crystal is greater than 70%. To the best of our knowledge, it is the highest value ever obtained for the FHG of Nd:YAG laser with a repetition rate of 10 Hz in low drive condition. G. Kruglik's¹⁰ reported that the conversion efficiency decrease with the increase of repetition rate. Typically, at the pulse repetition rate of 10 Hz, ~50% FHG conversion efficiency is obtained with a Nd:YAG laser. When the pulse repetition rate increases to 25 kHz, the conversion efficiency will drop to less than 4%.⁹

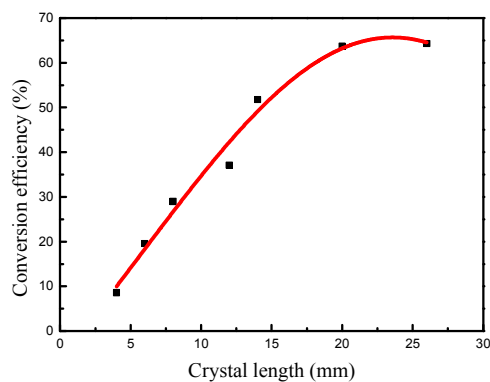


Figure 8. The highest FHG conversion efficiency of different length DKDP crystals.

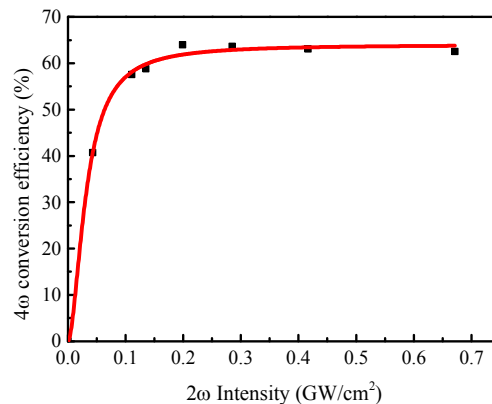


Figure 9. NCPM FHG conversion efficiency versus input 2ω intensity.

Conclusions

In summary, large sizes DKDP crystal ($100 \times 105 \times 96 \text{ mm}^3$) was grown by rapid growth method. The crystal quality is pretty good with the overall refractive index inhomogeneity below 0.441 ppm. NCPM FHG was realized at about $39.5 \sim 40^\circ\text{C}$, which indicated that the deuterium content of the crystal is extremely high (98.6~98.9%). The deuterium content distribution in this crystal is very homogeneous with only 0.14 %/cm deuterium gradient, which is much lower than the previously determined 0.59 %/cm in 75% deuterium content DKDP crystal. It is necessary to make the crystal within the laser spot range fixed at T_{NCPM} in order to obtain high FHG conversion efficiency. However, T_{NCPM} is sensitive to deuterium content. So deuterium homogeneity is important especially to large cross section high power laser system. Essentially, it is the extremely high deuterium content that makes it possible to gain better deuterium homogeneity, which further contributes to the efficient FHG. The FWHM of angular acceptance under NCPM condition is 10 times larger than that of critical phase-matching. The FHG conversion efficiency increases with the crystal length and reaches a flat top due to the absorption effect. The optimized crystal length is 20 mm or so, and the external FHG conversion efficiency is up to 64%. This method to gain high energy deep UV coherent light by homogeneous and high FHG conversion efficiency DKDP crystals can be widely used in precise material processing and spectroscopy fields in the future.

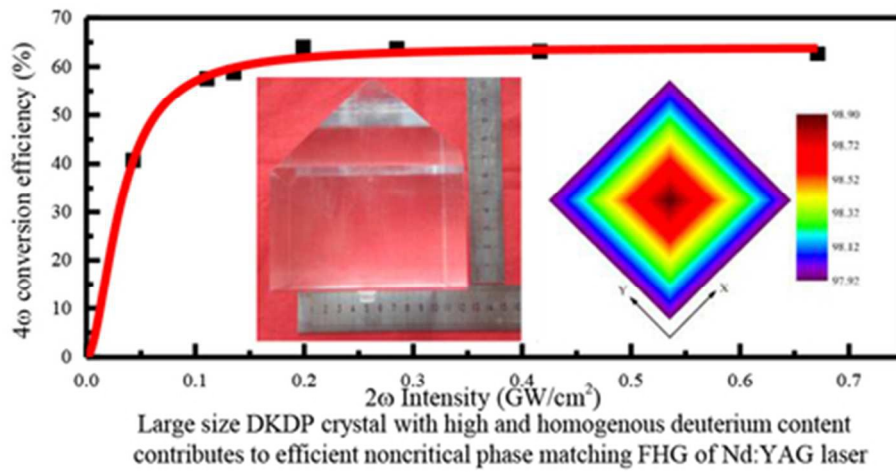
Acknowledgments

We would like to thank the kind support made by the National Natural Science Foundation of China (Grants No. 51323002, 51402173, and 61178060), the Ministry of Education (Grants No. 625010360) the Fundamental Research Funds of Shandong University (2015GN027) and the Key Laboratory of Neutron Physics, China Academy of Engineering Physics (Project 2014BB07).

Notes and references

- 1 C.T.Chen, *Laser Focus World*, 2004, **40**, 91-96.

- 2 Guerman Pasmanik, *Laser Focus World*, 2008, **44**, 105.
- 3 R. S. Adhav and R. W. Wallace, *IEEE Journal of Quantum Electronics*, 1973, **9**, 855.
- 4 K. KATO, *Optics Communications*, 1973, **9**(3), 249.
- 5 Liu, Y. S., Jones, W. B. and Chernoch, J. P., *Applied Physics Letters*, 1976, **29**(1), 32.
- 6 V. I. Bredikhin, V. N. Genkin, S. P. Kuznetsov and M. A. Novikov, *Sov. Tech. Phys. Lett.*, 1977, **3**, 165.
- 7 Gail A. Massey, Senior Member, IEEE, Michael D. Jones and Joel C. Johnson, *IEEE Journal of Quantum Electronics*, 1978, **14**(7), 527.
- 8 Michael D. Jones and Gail A. Massey, *IEEE Journal of Quantum Electronics*, 1979, **15**(4), 204.
- 9 P. E. Perkins and Theodore S. Fahlen, *IEEE Journal of Quantum Electronics*, 1985, **21**(10), 1636.
- 10 G. Kruglik, N. Kondratyuk and A. Shagov, *Proc. of SPIE*, 2002, **4751**, 137.
- 11 S. T. Yang, M. A. Hennessey and T. L. Weiland, et al., *Optics Letters*, 2011, **36**(10) 1824.
- 12 Shaohua Ji, Shaojun Zhang, Mingxia Xu, Baoan Liu, Lili Zhu, Lisong Zhang, Xinguang Xu, Zhengping Wang and Xun Sun, *Optical Materials Express*, 2012, **2**(6), 735.
- 13 Shaohua Ji, Fang Wang, Miaomiao Xu, Lili Zhu, Xinguang Xu, Zhengping Wang and Xun Sun, *Optics Letters*, 2013, **38**(10) 1679.
- 14 Shaohua Ji, Fang Wang, Lili Zhu, Xinguang Xu, Zhengping Wang and Xun Sun, *Scientific Reports*, 2013, **3**, 1605.
- 15 Wang Fang, Li Fu-quan, Chai Xiang-xu, Wang Li-quan, Han Wei, Jia Huai-ting, Zhou Li-dan, Feng Bin and Xiang Yong, *Proc. of SPIE*, 2015, **9255**, 92551R.
- 16 R. A. Phillips, *J. Opt. Soc. Am.*, 1966, **56**, 629.
- 17 M. Yamazaki and T. Ogawa, *J. Opt. Soc. Am.*, 1966, **56**, 1407.
- 18 N. P. Barnes, D.J. Gettemy and R.S. Adhav, *J. Opt. Soc. Am.*, 1982, **72**, 895.
- 19 G. C. Ghosh and G.C. Bhar, *IEEE Journal of Quantum Electronics*, 1982, **18**, 143.
- 20 Kevin W. Kirby and Larry G. DeShazer, *J. Opt. Soc. Am. B*, 1987, **4**(7), 1072.
- 21 Lisong Zhang, Guangwei Yu, Hailiang Zhou, Liang Li, Mingxia Xu, Baoan Liu, Shaohua Ji, Lili Zhu, Fafu Liu and Xun Sun, *Journal of Crystal Growth* 2014, **401**, 190.
- 22 D. Eimerl, L. Davis and S. Velsko, *Journal of Applied Physics*, 1987, **62** (5), 1968.
- 23 G. M. Loiacono; J. F. Balascio and W. Osborne, *Applied Physics Letters*, 1974, **24**, 455.
- 24 Shaohua Ji, Fuquan Li, Fang Wang, Xinguang Xu, Zhengping Wang and Xun Sun, *Optical Materials Express*, 2014, **4**(5), 997.



39x19mm (300 x 300 DPI)